

Coulomb blockade and non-Fermi-liquid behavior in quantum dots

Frithjof B. Anders,¹ Eran Lebanon,² and Avraham Schiller²

¹*Department of Physics, Universität Bremen, P.O. Box 330 440, D-28334 Bremen, Germany*

²*Racah Institute of Physics, The Hebrew University, Jerusalem 91904, Israel*

The non-Fermi-liquid properties of an ultrasmall quantum dot coupled to a lead and to a quantum box are investigated. Tuning the ratio of the tunneling amplitudes to the lead and box, we find a line of two-channel Kondo fixed points for arbitrary Coulomb repulsion on the dot, governing the transition between two distinct Fermi-liquid regimes. The Fermi liquids are characterized by different values of the conductance. For an asymmetric dot, spin and charge degrees of freedom are entangled: a continuous transition from a spin to a charge two-channel Kondo effect evolves. The crossover temperature to the two-channel Kondo effect is greatly enhanced away from the local-moment regime, making this exotic effect accessible in realistic quantum-dot devices.

PACS numbers: 73.23.Hk, 72.15.Qm, 73.40.Gk

Strongly correlated electron systems display non-Fermi-liquid properties in the vicinity of a zero-temperature phase transition.^{1,2} In lattice systems, the nature of these so-called quantum critical points is still not well understood. While theoretical descriptions typically start from well-defined quasiparticle excitation modes, the non-Fermi-liquid behavior is interaction driven, and arises from persisting quantum-mechanical fluctuations between these modes.^{1,2} The two-channel Kondo effect (2CKE) is a prototype for such a quantum critical point in a quantum impurity system. It occurs when a spin- $\frac{1}{2}$ local moment is coupled antiferromagnetically with equal strength to two independent conduction-electron channels that overscreen the moment.³ Its fixed point governs the transition between two distinct Fermi liquids, which are adiabatically connected at finite temperature. While certain ballistic metallic point contacts, two-level systems, and heavy fermion alloys have been argued to display the 2CKE,³ a conclusive experimental observation of this elusive effect remains lacking.

Quantum-dot devices have become an important tool for investigating fundamental questions such as the 2CKE, since they allow for detailed sample engineering and direct control of the microscopic model parameters. Here we investigate realizations of the 2CKE in a double-dot device, comprised of a quantum box (i.e., a large dot) indirectly coupled to a lead via an ultrasmall quantum dot.⁴ In the Coulomb-blockade valleys, charge fluctuations are suppressed on the quantum box. This blocks the interlead exchange coupling at temperatures below the charging energy of the box, thereby generating two independent screening channels for the local moment formed on the small dot.⁵ A spin 2CKE then develops on the dot if the effective spin-exchange couplings to the lead and box are tuned to be equal.⁵ So far, only the local-moment regime was considered within this scenario.^{5,6,7}

In this paper, we explore different regimes of the lead-dot-box device, where charge is not quantized on the quantum dots. We find the following: (i) a line of two-channel fixed points as a function of the gate voltages in the device, extending to the mixed-valent regime of the ultrasmall dot and away from the Coulomb-blockade val-

leys of the quantum box; (ii) a continuous transition from a spin 2CKE to a charge 2CKE for an asymmetric dot; (iii) an intriguing entanglement of spin and charge within the 2CKE that develops in the experimentally relevant case of particle-hole asymmetry, reflected in a simultaneous $\ln(T)$ divergence of the magnetic susceptibility of the dot and the charge capacitance of the box; (iv) an abrupt jump in the $T = 0$ conductance across the two-channel line. Here the Fermi liquids on either side of the critical line are characterized by distinct values of the $T = 0$ conductance.

The setting we consider consists of an ultrasmall quantum dot, modeled by a single energy level ϵ_d and an on-site repulsion U , embedded between a metallic lead and a quantum box. The quantum box is characterized by a finite charging energy, E_C , and by a dense set of single-particle levels, which we take to be continuous. Denoting the creation of an electron with spin projection σ on the dot by d_σ^\dagger , the corresponding Hamiltonian reads

$$\mathcal{H} = \sum_{\alpha=L,B} \sum_{k,\sigma} \epsilon_{\alpha k} c_{\alpha k \sigma}^\dagger c_{\alpha k \sigma} + E_C (\hat{n}_B - N_B)^2 \quad (1)$$

$$+ \epsilon_d \sum_{\sigma} d_\sigma^\dagger d_\sigma + U \hat{n}_{d\uparrow} \hat{n}_{d\downarrow} + \sum_{\alpha,k,\sigma} t_\alpha \left\{ c_{\alpha k \sigma}^\dagger d_\sigma + \text{H.c.} \right\},$$

where $c_{Lk\sigma}^\dagger$ ($c_{Bk\sigma}^\dagger$) creates a lead (box) electron with momentum k and spin projection σ , t_L (t_B) is the tunneling matrix element between the quantum dot and the lead (box), ϵ_{Lk} (ϵ_{Bk}) are the single-particle levels in the lead (box), and $\hat{n}_{d\sigma}$ equals $d_\sigma^\dagger d_\sigma$. The excess number of electrons inside the box, $\hat{n}_B = \sum_{k\sigma} [c_{Bk\sigma}^\dagger c_{Bk\sigma} - \theta(-\epsilon_{Bk})]$, is controlled by the dimensionless gate voltage, N_B .

We treat the Hamiltonian of Eq. (1) using a recent adaptation of Wilson's numerical renormalization-group (NRG) method⁸ to the Coulomb blockade.⁹ Introducing three collective charge operators for the box,¹⁰ $\hat{N} = \sum_{m=-\infty}^{\infty} m|m\rangle\langle m|$ and $\hat{N}^\pm = \sum_{m=-\infty}^{\infty} |m \pm 1\rangle\langle m|$, we replace the tunneling term between the dot and the box in Eq. (1) with $\sum_{k,\sigma} t_B \left\{ \hat{N}^+ c_{Bk\sigma}^\dagger d_\sigma + \text{H.c.} \right\}$, while the charging-energy term is converted to $E_C (\hat{N} - N_B)^2$.

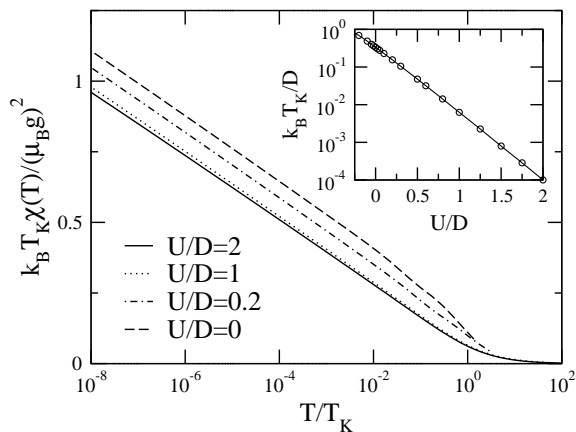


FIG. 1: The magnetic susceptibility of the dot vs T , for $\Gamma_L = E_C = 0.1D$, $N_B = 0$, and different values of $U = -2\epsilon_d$. Here Γ_B is tuned for each value of U to the two-channel point $\Gamma_B^{2\text{CK}}$. The Kondo temperature T_K is defined in Eq. (2). For all U , ranging from the local-moment regime $U \gg \Gamma_L$, to the strongly mixed-valent regime $U = 0$, to negative U (not shown), there exists a two-channel point $\Gamma_B^{2\text{CK}}$ where $\chi(T)$ diverges logarithmically as $T \rightarrow 0$, and the finite-size spectrum converges to the conventional two-channel fixed point. Inset: T_K vs U . For $U \gg \Gamma_L, E_C$ (local-moment regime), T_K decreases exponentially with U . For $U < \Gamma_L$ (mixed-valent regime), it exceeds E_C .

Since the dynamics of \hat{N} is insensitive to the precise number of conduction electrons in the bands, one can relax the constraint $\hat{N} = \hat{n}_B$, and regard \hat{N} as an independent degree of freedom.⁹ The resulting Hamiltonian describes then two noninteracting conduction bands coupled to a complex impurity, composed of both \hat{N} and the dot degrees of freedom. Taking the two conduction baths to have a common rectangular density of states, $\rho(\epsilon) = \rho\theta(D - |\epsilon|)$, we solve the resulting model using the NRG. Here the number N_s of NRG states retained sets a lower bound on the ratio E_C/D one can treat. Throughout the paper we set the NRG discretization parameter⁸ Λ equal to 2.8, while $N_s = 2000$.

We begin with a symmetric dot, $U = -2\epsilon_d$, and with a box tuned to the middle of a Coulomb-blockade valley, $N_B = 0$. Fixing E_C and the hybridization strength to the lead, $\Gamma_L = \pi\rho t_L^2$, we varied the hybridization to the box, $\Gamma_B = \pi\rho t_B^2$, in search of a 2CKE. Our results for $E_C = \Gamma_L = 0.1D$ are summarized in Fig. 1. Quite surprisingly, we find a two-channel Kondo point $\Gamma_B^{2\text{CK}}$ for all values of U , ranging from the local-moment regime $U \gg \Gamma_L$, to the strongly mixed-valent regime $U \approx 0$, to the unrealistic regime of $U < 0$. The development of a 2CKE is reflected in a logarithmic divergence of the dot susceptibility¹¹ as $T \rightarrow 0$ (see Fig. 1), and in a finite-size spectrum that converges to the conventional two-channel fixed point (i.e., identical energies, degeneracies, and quantum numbers).

The emergence of a spin 2CKE for $U \gg \Gamma_L$ proves the scenario of Ref. 5. Specifically, the associated Kondo temperature decays exponentially with U for $U \gg$

Γ_L, E_C (inset of Fig. 1), while the ratio $\Gamma_B^{2\text{CK}}/\Gamma_L$ approaches the asymptotic value $1 + 2E_C/U$ (not shown). Here and throughout the paper we define the Kondo temperature T_K according to the Bethe ansatz expression for the slope of the $\ln(T)$ diverging term in the susceptibility of the two-channel Kondo model,¹²

$$\chi(T) \sim \frac{(\mu_B g)^2}{20k_B T_K} \ln(T_K/T). \quad (2)$$

We emphasize, however, that our NRG calculations go well beyond the Schrieffer-Wolff transformation used in Ref. 5, confirming that no relevant perturbations are generated at higher orders in the tunneling amplitudes.

Contrary to the local-moment regime, the development of a spin 2CKE in the mixed-valent regime (let alone for $U < 0$) is an unexpected feature, with no apparent spin degree of freedom to be overscreened. Moreover, T_K is significantly enhanced for $U \approx 0$, exceeding E_C in Fig. 1. This behavior is reminiscent of the two-channel Anderson model, where the 2CKE likewise persists into the mixed-valent regime.¹³ Particularly intriguing is the limit of a noninteracting dot, which reduces⁴ to the familiar problem of a quantum box connected to a lead by single-mode tunneling. Although a charge 2CKE was predicted for the latter setting at the degeneracy points of the Coulomb blockade,¹⁴ no spin 2CKE was previously anticipated.

To understand the 2CKE for $U = 0$, we revisit the problem of a quantum box connected to a lead by a nearly fully transmitting single-mode point contact. Following Refs. 15 and 16, we model this system by a one-dimensional (1D) geometry, where $x < 0$ ($x > 0$) represents the lead (box), and $x = 0$ corresponds to the noninteracting dot. The deviation from perfect transmission is modeled^{15,16} by weak backscattering at $x = 0$. Extending the bosonization treatment of Ref. 16 to a finite local magnetic field acting on the dot, and carefully accounting for an underlying symmetry of the Hamiltonian,¹⁷ we obtain the following linear magnetic susceptibility for $k_B T \ll E_C$:

$$\chi(T) = \chi_0 \left(\frac{\mu_B g}{\hbar v_F} \right)^2 \left[\ln \left(\frac{D_{\text{eff}}}{2\pi k_B T} \right) - \psi \left(\frac{1}{2} + \frac{\Gamma}{2\pi k_B T} \right) \right], \quad (3)$$

where $\chi_0 = \Gamma/(4\pi R)$ and $\Gamma = R(8\gamma E_C/\pi^2) \cos^2(\pi N_B)$. Here, R is the reflectance, v_F is the Fermi velocity, γ equals e^C with $C \approx 0.5772$, $\psi(x)$ is the digamma function, and D_{eff} is an effective cutoff of the order of E_C .

Equation (3) features a logarithmic temperature dependence down to $k_B T \sim \Gamma$. Hence, $\chi(T)$ diverges logarithmically for perfect transmission, when $\Gamma \propto R$ vanishes. In fact, $\chi(T)$ diverges logarithmically at perfect transmission for all gate voltages, except for half-integer values of N_B where χ_0 vanishes. In particular, Eq. (3) predicts $T_K(N_B) \propto 1/\cos^2(\pi N_B)$.

Equation (3) formally describes the limit $E_C \ll \Gamma_L$, since Γ_L serves as the effective bandwidth for the 1D model used (see Ref. 4, Sec. III). Surprisingly, we find

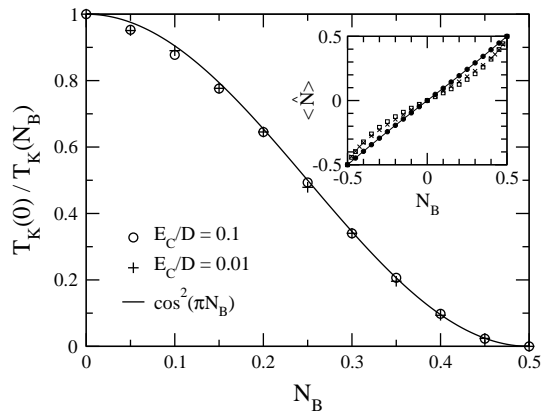


FIG. 2: $1/T_K$ vs N_B for $U = \epsilon_d = 0$ and $\Gamma_L/D = 0.1$. Here E_C/D equals 0.1 (circles) and 0.01 (pluses). For each combined value of N_B and E_C , the coupling Γ_B is tuned to the two-channel point $\Gamma_B^{2\text{CK}}$. As a function of N_B , $\Gamma_B^{2\text{CK}}(N_B)$ varies by less than 0.2% for each fixed value of E_C . The ratio $T_K(0)/T_K(N_B)$ is well described by $\cos^2(\pi N_B)$ (solid line). Inset: The box charge $\langle \hat{N} \rangle$ vs N_B for $\Gamma_L = E_C = 0.1D$ and $U = \epsilon_d = 0$. Here Γ_B/Γ_L equals 1 (squares), 1.72 (filled circles + solid line), and 3.24 (crosses). The Coulomb staircase is completely washed out for $\Gamma_B = \Gamma_B^{2\text{CK}}(0) = 1.72\Gamma_L$, but is gradually recovered upon departure from $\Gamma_B^{2\text{CK}}(0)$.

good agreement with the NRG results for $U = 0$ even for E_C as large as Γ_L . (i) Scanning N_B for fixed E_C and Γ_L , we find a 2CKE for all gate voltages, with a Kondo temperature that varies as $T_K(N_B) \propto 1/\cos^2(\pi N_B)$ (Fig. 2). (ii) Consistent with the notion of perfect transmission, only small variations are found in $\Gamma_B^{2\text{CK}}(N_B)$ as a function of N_B (less than 0.2%), falling within our numerical precision. (iii) The Coulomb staircase in the charging of the box is washed out for $\Gamma_B = \Gamma_B^{2\text{CK}}(0)$, but is gradually recovered as Γ_B sufficiently departs from $\Gamma_B^{2\text{CK}}(0)$, whether above or below (inset of Fig. 2). (iv) Upon reducing E_C/Γ_L from 1 to 0.081, the ratio $\Gamma_B^{2\text{CK}}(0)/\Gamma_L$ steadily decreases from 1.72 to 1.11. This suggests the limit $\Gamma_B^{2\text{CK}} \rightarrow \Gamma_L$ as $E_C \rightarrow 0$, matching the condition for perfect transmission for two noninteracting leads. Thus, the spin 2CKE for $U = 0$ is well described by Eq. (3).

So far we have considered a symmetric dot, and varied $U = -2\epsilon_d$. In reality, however, U is large and fixed. The experimentally tunable parameters are the dot level ϵ_d , the dimensionless gate voltage N_B , and, to a lesser degree, the tunneling rates Γ_L and Γ_B . In Figs. 3 and 4 we explore the 2CKE as a function ϵ_d , for $U/D = 2$ and $\Gamma_L = E_C = 0.1D$. Figure 3(a) shows the two-channel line $\Gamma_B^{2\text{CK}}/\Gamma_L$ versus ϵ_d , for $N_B = 0$. The two-channel line separates two distinct Fermi liquids, where the dot is coupled more strongly to the box (for Γ_B above the line) or to the lead (below and to the side of the line). Deep in the local-moment regime there is good agreement with the estimate of Ref. 5 based on the Schrieffer-Wolff transformation (dashed line). However, large deviations develop as one approaches the mixed-valent regime.

Fixing Γ_B at the $N_B = 0$ value of $\Gamma_B^{2\text{CK}}$, the shape of

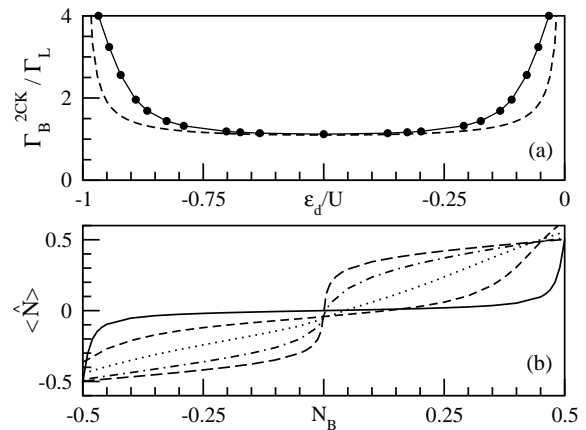


FIG. 3: (a) The two-channel line $\Gamma_B^{2\text{CK}}/\Gamma_L$ vs ϵ_d for $U/D = 2$, $\Gamma_L = E_C = 0.1D$, and $N_B = 0$. Dashed line: The local-moment estimate of Ref. 5. (b) The charge curve $\langle \hat{N} \rangle$ vs N_B , for $\epsilon_d/D = -1, -1.581, -1.733, -1.843$, and -1.935 (solid, dashed, dotted, dot-dashed, and long-dashed line, respectively). For each value of ϵ_d , Γ_B is tuned to the corresponding $N_B = 0$ value of $\Gamma_B^{2\text{CK}}$, depicted in panel (a).

the charge step dramatically changes upon going from the local-moment to the mixed-valent regime [see Fig. 3(b)]. For $\epsilon_d = -U/2$, one recovers a conventional Coulomb-blockade staircase, with charge plateaus at integer units of charge. Upon decreasing ϵ_d , the Coulomb staircase is gradually smeared, until it is essentially washed out for $\epsilon_d/D \approx -1.73$. Upon further decreasing ϵ_d , there is a reentrance of the Coulomb staircase. However, the

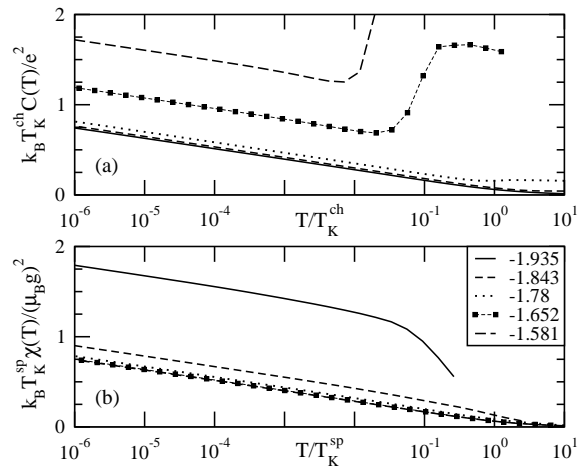


FIG. 4: (a) The capacitance of the box and (b) the magnetic susceptibility of the dot, for $U/D = 2$, $\Gamma_L = E_C = 0.1D$, $N_B = 0$, and different values of ϵ_d/D , as specified in the legends. For each ϵ_d , Γ_B is tuned to the corresponding $N_B = 0$ value of $\Gamma_B^{2\text{CK}}$. Both $\chi(T)$ and $C(T)$ diverge logarithmically as $T \rightarrow 0$, but with different Kondo scales T_K^{sp} and T_K^{ch} , extracted from the slopes of the $\ln(T)$ diverging terms. In going from $\epsilon_d/D = -1.581$ to $\epsilon_d/D = -1.935$, $k_B T_K^{\text{sp}}/D$ takes the values 0.0022, 0.0054, 0.0457, 0.187, and 1.72, while $k_B T_K^{\text{ch}}/D$ equals 1.035, 0.36, 0.035, 0.009, and 0.00138, respectively.

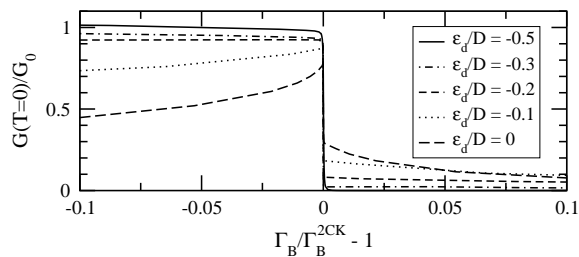


FIG. 5: The zero-temperature conductance of the two-lead device proposed in Ref. 5, for $U/D = 1$, $E_C/D = 0.1$, $N_B = 0$, and different values of ϵ_d . The tunneling rates Γ_l and Γ_r are kept fixed in all curves, with $\Gamma_l + \Gamma_r = 0.1D$. Here $G_0 h/2e^2$ equals $4\Gamma_l\Gamma_r/(\Gamma_l + \Gamma_r)^2$.

degeneracy points are shifted to integer values of N_B , and the charge plateaus occur at half-integer units of charge.

To understand this surprising shift of the Coulomb staircase, we note that it happens for Γ_B^{2CK} several times larger than Γ_L and E_C . We therefore diagonalize first the local problem of the dot and the two box degrees of freedom directly coupled to it, before incorporating the smaller scales Γ_L and E_C . For $U \gg t_B \gg U + \epsilon_d$, the ground state of the local problem is a strong admixture of the dot and box degrees of freedom, whose respective occupancies are $3/2$ and $1/2$. Switching on E_C , the remaining box degrees of freedom not directly coupled to the dot thus experience an effective charging-energy interaction similar to that of Eq. (1), but with N_B shifted by half an integer. The resulting integer charge plateaus for the remaining box degrees of freedom translate then to half-integer charge plateaus for the entire box.

The most striking feature of particle-hole asymmetry is the entanglement of spin and charge within the 2CKE that develops. As demonstrated in Fig. 4 for $N_B = 0$ and different values of $\epsilon_d \neq -U/2$, there is a simultaneous $\ln(T)$ divergence of the dot susceptibility $\chi(T)$ and the box capacitance $C(T) = (e^2/2E_C)d\langle\hat{N}\rangle/dN_B$, when Γ_B is tuned to the corresponding $N_B = 0$ value of Γ_B^{2CK} . Hence, the resulting 2CKE is neither of pure spin nor of pure charge character, but rather involves both sectors. Quite remarkably, the degeneracy point where $C(T \rightarrow 0)$ diverges is pinned at $N_B = 0$ for all ϵ_d , although the charge curves of Fig. 3(b) show no particular symmetry about this point. Moreover, there are two distinct Kondo scales, T_K^{sp} and T_K^{ch} , extracted from the slopes of the $\ln(T)$ diverging terms in $\chi(T)$ and $C(T)$. Upon decreasing ϵ_d from $-U/2$ to $-U$, T_K^{sp} monotonically increases while T_K^{ch} monotonically decreases. This marks a continuous transition from a predominantly spin 2CKE

deep in the local-moment regime, to a predominantly charge 2CKE, reminiscent of Matveev's scenario,^{4,14} in the strongly mixed-valent regime.

Experimentally, the relevant temperature scale is the crossover temperature T_0 , below which the 2CKE sets in. Estimating T_0 from the NRG level flow, we find that it roughly traces $T_{\min} = \min\{T_K^{sp}, T_K^{ch}\}$. The latter scale is greatly enhanced when spin and charge are strongly entangled, reaching a maximum of $k_B T_{\min} \sim 0.4E_C$ for the model parameters of Fig. 4. Hence, the conditions for observing the 2CKE in realistic quantum-dot devices are most favorable when the spin and charge degrees of freedom are strongly entangled.

The dot susceptibility is very useful theoretically for analyzing the 2CKE, but difficult to measure for a single dot. In Fig. 5 we depict the $T = 0$ conductance, $G(0)$, for the two-lead device proposed in Ref. 5. Here the single lead is replaced with two separate leads, characterized by the tunneling rates Γ_l and Γ_r . In equilibrium, this setting is equivalent⁵ to a single lead with $\Gamma_L = \Gamma_l + \Gamma_r$. At $T = 0$, the conductance is proportional to the dot spectral function at the Fermi energy, which we calculate using the NRG. Fixing Γ_l and Γ_r , $G(0)$ drops abruptly as Γ_B crosses Γ_B^{2CK} . However, in contrast to the treatment of Ref. 6, the height of the conductance step is not fixed. It decreases in size with increasing charge fluctuations on the dot. Indeed, away from the Kondo limit $G(0)$ neither vanishes for $\Gamma_B > \Gamma_B^{2CK}$ nor reaches the unitary limit for $\Gamma_B < \Gamma_B^{2CK}$. In the mixed-valent regime, $G(0)$ actually develops a maximum at $\Gamma_B = \Gamma_B^{2CK} + 0^-$, reflecting the crossover to a Matveev-type charge 2CKE.

In summary, we found a line of two-channel fixed points in a double-dot device, characterized by the number of excess electrons in the box and by the ratio of the tunneling rates. These fixed points govern the crossover from one Fermi liquid to another, and are experimentally detectable by a sharp drop in the conductance. Charge and spin degrees of freedom are generally entangled, and decouple only at special particle-hole symmetry points such as $N_B = 0$ and $\epsilon_d = -U/2$. The crossover temperature to the two-channel Kondo effect is greatly enhanced away from the local-moment regime, making this exotic effect accessible in realistic quantum-dot devices.

We have benefited from fruitful discussions with L. Glazman, D. Goldhaber-Gordon, Y. Oreg, D. Orgad, and R. Potok. E.L. and A.S. were supported in part by the Centers of Excellence Program of the Israel Science Foundation. F.B.A. acknowledges funding of the NIC, Forschungszentrum Jülich, under Project No. HHB00.

¹ J. A. Hertz, Phys. Rev. B **14**, 1165 (1976).

² A. J. Millis, Phys. Rev. B **48**, 7183 (1993).

³ For a comprehensive review, see D. L. Cox and A. Zawadowski, Adv. Phys. **47**, 599 (1998).

⁴ E. Lebanon *et al.*, Phys. Rev. B, **68**, 155301 (2003)

⁵ Y. Oreg and D. Goldhaber-Gordon, Phys. Rev. Lett. **90**, 136602 (2003).

⁶ M. Pustilnik *et al.*, Phys. Rev. B **69**, 115316 (2004).

- ⁷ S. Florens and A. Rosch, Phys. Rev. Lett. **92**, 216601 (2004).
- ⁸ K. G. Wilson, Rev. Mod. Phys. **47**, 773 (1975).
- ⁹ E. Lebanon *et al.*, Phys. Rev. B **68**, 041311 (2003).
- ¹⁰ J. König and H. Schoeller, Phys. Rev. Lett. **81**, 3511 (1998).
- ¹¹ The dot susceptibility was computed from the dot magnetization for a small local magnetic field.
- ¹² P. D. Sacramento and P. Schlottmann, Phys. Lett. A **142**, 245 (1989).
- ¹³ A. Schiller *et al.*, Phys. Rev. Lett. **81**, 3235 (1998); C. J. Bolech and N. Andrei, *ibid.* **88**, 237206 (1998).
- ¹⁴ K. A. Matveev, Zh. Eksp. Teor. Fiz. **99**, 1598 (1991) [Sov. Phys. JETP **72**, 892 (1991)].
- ¹⁵ K. Flensberg, Phys. Rev. B **48**, 11156 (1993).
- ¹⁶ K. A. Matveev, Phys. Rev. B **51**, 1743 (1995).
- ¹⁷ Details of the calculation will be published elsewhere.